1347 Pathologic Studies of Leptospirosis, Ten-Years Experience at Centers for Disease Control and Prevention

W-J Shieh, P Chris, J Guarner, SR Zaki. Centers for Disease Control and Prevention, Atlanta, GA; Children's Hospital of Atlanta, Emory University, Atlanta, GA.

Background: Leptospirosis is a zoonotic disease caused by spirochetes of the genus *Leptospira*. It is a common infection affecting many species of wild and domestic animals worldwide. Human infection can occur either through direct contact with infected animals or more commonly through indirect contact with water or soil contaminated with the urine of infected animals. Pathologic studies are rarely performed and the pathogenesis of leptospirosis remained largely unknown.

Design: One hundred and sixty-five cases with positive immunohistochemical (IHC) test results for leptospira were identified from 1998–2008 database at Infectious Disease Pathology Branch, CDC. Although a few cases were from the US, most came from South America, Central America, and South East Asia. Histopathologic evaluation on available tissue samples was performed. The IHC assay was an indirect immunoalkaline phosphatase technique with a mixture of 16 rabbit polyclonal anti-leptospira antisera. Steiner's silver stain was also performed on selected cases.

Results: Histopathologic changes in the liver included hyperplasia of Kupffer cells, mild to moderate inflammatory infiltrate in portal tracts, and occasional hepatocellular necrosis. The lung frequently showed prominent intra-alveolar hemorrhage. The most consistent histopathology was a diffuse tubulointerstitial inflammation in the kidney, characterized by a mixed infiltrate of inflammatory cells. Although silver stains can highlight leptospires in tissues, they were not able to demonstrate fragments of bacteria disintegrated by host response or antibiotics treatment. IHC assay readily demonstrated granular, short filamentous, or spirochetal immunostaining of bacterial antigens, and is more useful for diagnosis.

Conclusions: The diagnosis of leptospirosis suspected by history and clinical manifestations can be supported by histopathologic findings, including interstitial nephritis and pulmonary hemorrhage. However, these features can occur in a variety of viral and bacterial infections. Silver stains are generally not a sensitive method for diagnosis because the detection of leptospires can be confounded by duration of illness and antibiotics treatment. IHC assay can detect leptospiral antigens in tissues and is a more sensitive and specific method for diagnosis. It is also instrumental for the studies of pathogenesis of leptospirosis.

1348 Activated Protein C Substantially Improves Survival in a Baboon Model of Anthrax-Mediated Sepsis

DJ Stearns-Kurosawa, V Collins, S Freeman, S Kurosawa. Boston University School of Medicine, Boston, MA.

Background: A fulminant septic response contributes to the lethality of toxigenic, Gram positive, *Bacillus anthracis*, the cause of clinical anthrax, but few studies address adjunctive therapeutics that might influence disease severity and mortality after infection. In ongoing studies, this model recapitulates the coagulopathic, inflammatory and metabolic pathophysiological changes in a manner similar to humans, with the lung as a primary target organ. The current study evaluates whether pre-treatment with recombinant activated protein C, a potent anti-coagulant and anti-inflammatory drug, influences outcome or disease severity in this model of anthrax bacteremia.

Design: Anesthetized nonhuman primates (*Papio c. cynocephalus*; n=40; 6-8kg) were pre-treated with recombinant activated protein C (DAA, drotrecogin alfa (activated)) followed by challenge with i.v. bacteria infusion. Some baboons were challenged with *B.anthracis* Sterne strain which produces anthrax toxins (n=32; toxemia + sepsis); some were challenged with *B.anthracis* Delta Sterne strain which does not produce toxins (n=8; sepsis only). The effect of DAA on baboon septic responses was determined by monitoring on-line physiologic responses, inflammation, coagulation, organ responses and survival.

Results: All baboons challenged with lethal doses of *B. anthracis* Delta Sterne strain survived as a result of DAA treatment ($p<0.01$). Challenge with Delta Sterne strain induced a typical septic response and DAA pre-treatment was accompanied by reduced coagulopathy, inflammation and pulmonary injury. The influence of DAA pre-treatment on animal responses after challenge with toxigenic Sterne strain was related to whether lethality was driven by sepsis or acute pulmonary injury. DAA ameliorated the later responses (>24hrs) due to sepsis and these animals survived ($p<0.05$), but treatment did not influence the early pulmonary failure (<24 hrs) which may be governed by exotoxin activities.

Conclusions: Death due to infection with *B. anthracis* is governed by both septic responses and the activities of anthrax exotoxins. Pre-treatment with DAA was highly effective in preventing death due to anthrax-mediated sepsis, but did not alter the very early deaths that may be attributable to exotoxins and/or other bacterial virulence factors. Thus, an effective therapeutic approach for treatment of *B.anthracis* infection will need to provide relief for the pathogenic effects of both anthrax toxins and host septic responses. [NIH RO1AI058107, U19AI062629 (SK)]

1349 Sepsis Induces Extensive Autophagy and Mitochondrial Damage in Human and Mouse Liver

PE Swanson, E Watanabe, JT Muenzer, RS Hotchkiss. University of Washington, Seattle, WA; Washington University, St. Louis, MO.

Background: Autophagy is a regulated process by which a cell degrades and recycles its own components; it can be triggered as an adaptive response during times of stress. Incorporation of organelles and cytoplasm into lysosomes (autolysosomes/autophagosomes) constitutes morphologic evidence of this process. The purpose of this study was to determine to what extent organellar damage and autophagy occurs in hepatocytes during sepsis.

Design: Electron microscopy (EM) was performed on post-mortem liver samples from 6 septic patients (obtained within 90 minutes of death) and from 4 control patients who had elective liver resection. Liver specimens were also obtained 24 hours after surgery from 4 sham-operated mice and 4 mice with sepsis surgery (cecal ligation and puncture - CLP). All samples were fixed and processed in a routine fashion. The number of autophagosomes was derived from 2500x magnification survey images (~3000 μ^2) to avoid sample bias; counts were performed in a blinded fashion on randomly sequenced images. Patterns of organellar injury were based on higher magnification images (15000-40000x) that were biased in favor of abnormal findings.

Results: Autophagosomes were more numerous in septic patients: 5.3 ± 3.3 vs. 1.2 ± 1.5 (mean ± SD) autophagosomes per image in sepsis vs. controls, respectively ($p<0.001$). Mitochondrial membrane abnormalities, including herniation of outer membranes into adjacent organelles, vacuolar change in cristae and myelin figures were seen in sepsis samples, but not controls. Nuclei and other hepatocyte organelles showed no consistent abnormality. Residual bodies were not more common in sepsis. Murine sepsis paralleled human studies, with 38.7 ± 3.9 and 7.2 ± 1.9 autophagosomes in septic and sham mice, respectively ($p = 0.002$). Autophagosomes incorporated lipid droplets in murine, but not human, samples. Neither necrotic nor apoptotic cell death was observed.

Conclusions: Hepatocyte autophagosomes are increased during sepsis in both humans and mice. The reproducible presence of mitochondrial membrane changes suggests both a source of organellar material in sepsis-induced autophagy and an underlying pattern of sepsis-related cell injury. The similarities between human and murine samples emphasizes the value of murine CLP-induced sepsis as a model of human disease.

Informatics

1350 Utility of VIPER (Virtual Imaging for Pathology, Education & Research) in Continuing Medical Education and Slide Surveys

T Barr, K Nicol, D Billiter, K Wohlever, P Baker, V Prasad. Nationwide Children's Hospital, Columbus, OH; Ohio Supercomputer Center, Columbus, OH.

Background: Current slide survey programs utilize glass slides for continuing medical education and are fraught with challenges. Examples include difficulty obtaining, cutting, staining, and shipping of multiple glass slides, inability to annotate slides and potential for discrepancy among slides due to loss of tissue in deeper sections. Digital pathology systems provide high-quality images that correspond to entire glass slides and provide image quality equivalent to a microscope. Use of digital pathology in teaching venues addresses these issues with slides by reducing the quantity of tissue and slides required, permitting multiple annotations and allowing all participating pathologists to review the same image.

Design: Virtual Imaging for Pathology, Education, & Research (VIPER) is a web-based application designed to facilitate digital reviews of whole slide images, providing an interface to whole slide images, pathology reports, and custom forms. Same images can be viewed independently or simultaneously. VIPER utilizes a relational database system capturing review data, generating multiple reports of interest. VIPER Team has partnered with a Supercomputer Center which contains an infrastructure providing high capacity data storage, a high performing network, and the ability to access high performance computing. We have had success with in-house pathologist review of web based images.

Results: There are challenges with established working groups adapting to new technology. Minimal training quickly improved the acceptance and comfort in utilizing digital images rather than the microscope and glass slides.

Conclusions: Benefits of providing high quality digital images in a custom application for educational prevails over traditional methods as it is cost effective. Digital technology enhances the learning experience by allowing multiple annotations as well as allowing multiple users to view the same image from different physical locations simultaneously. The use of VIPER is already creating a digital archive of clinically annotated data sets providing continued value to the pathology community. In the future these data sets could be utilized for continuing medical education, pathology reviews and research.

1351 Case of the Month and the Virtual Slidebox Implementation

V Brodsky, A Louissaint, J Gilbertson, Y Yagi. Massachusetts General Hospital, Boston, MA.

Background: Currently, a large volume of surgical pathology cases deemed interesting and often received from different countries are reviewed during the daily "Outs" conference with the residents and fellows of the Massachusetts General Hospital's Pathology department. These slides are subsequently filed for storage or returned to sender and are not necessarily easily retrievable for later review. We have built a searchable database driven collection of whole slide images of the slides presented at these conferences, accessible via a web interface. Additionally, selected surgical pathology cases with the associated added clinical history are submitted into a queue by the residents, with one case picked and published monthly on the "Case of the Month" website.

Design: The development platform corresponding with the Massachusetts General Hospital website includes Microsoft Windows Server 2008 and Microsoft SQL Server Developer Edition. The Case of the Month website is built on the open source ASP-based Blogengine 1.4 with modifications allowing for submission queuing prior to final approval. The slides are scanned with 0.33um/pixel sampling period using Mirax Scan device (3DHISTECH Ltd, Carl Zeiss Microimaging GmbH) and are put on a dedicated storage server, each linked from the 3DHISTECH's Mirax Server database software, which provides its own Virtual Slidebox web interface as well as allowing for links from the Case of the Month website to target individual slides. Clicking on the link to the whole slide image in the browser opens the Mirax Viewer which lets the user navigate the whole slide image streaming from the server.

Results: The interactions with the scanner and the website are currently agreed to be valuable additions to the resident education. The 0.33um/pixel sampling period of the scanned slides appears sufficient for surgical cases and is considerably higher than the resolution of printed histological atlases, however the possibility of scanning cytology

slides at higher resolution is being considered.
Conclusions: Providing the searchable and easily navigable web database of whole slide images is definitely appreciated by the residents as an educational resource. We are collecting the usage data and will be investigating the possibility of opening access to the Harvard medical students and the outside world. The latter may prove to be a challenging task considering the bandwidth necessary to serve whole slide images. Eventual tracking of viewing patterns within the image will help identify high-yield areas important for diagnosis.

1352 Tumor Pathology Report in 3D Dynamic Image Format

B Castaneda, D Hosey, J Strang, DJ Rubens, KJ Parker, J Yao, Z Qu. University of Rochester, Rochester, NY.
Background: Tumor pathology reports are a critical component in the clinical management of cancer patients. Currently, pathology reports of malignant neoplasm remain in text format with the occasional presence of selected 2D still images for marketing purposes. Images are considered the most comprehensive and intuitive form of information for morphological abnormalities. In this abstract, we propose and report a 3D image pathology reporting module using prostate as a model that allows direct and visual assessment of several critical tumor attributes such as size, volume, shape, location, extent and margin status.
Design: Intact prostate glands with carcinoma were received after radical prostatectomy. A landmark device, which consisted of two sets of four (3 mm diameter) mating metal prongs, was inserted into the specimen through the apex and base to provide fiducial markers for 3D reconstruction. Subsequently, a whole-mount protocol was followed and complete serial sections (4mm apart) were mounted on 70 x 50 mm slides and stained by routine H&E for microscopic evaluation. The carcinoma was outlined in the slides. Image segmentation techniques were used to extract the contours of the gland and the tumor. These contours were interpolated to create a 3D model which was dynamically visualized using a web interface.
Results: Figure 1 illustrates the implemented web interface showing a 3D model of the prostate gland (cyan) and the carcinoma (red). Users can access this interface to view a colored 3-D model of a tumor from several angles to reveal the tumor size, shape and location in the specimen.

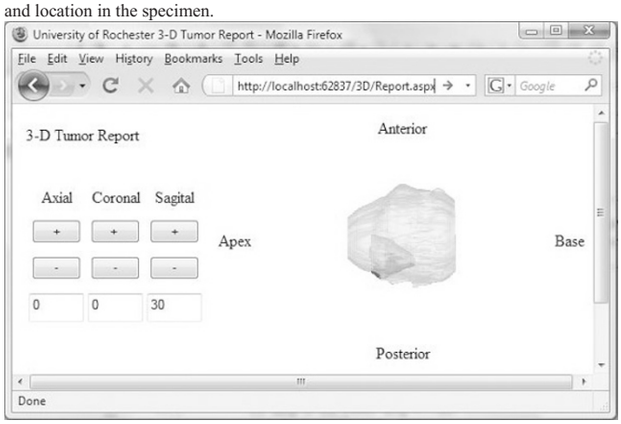

Conclusions: We propose a 3D pathology tumor report by combining well established pathology specimen whole-mount methods, image processing techniques, and 3D modeling software tools. This reporting method allows for a more comprehensive appreciation and assessment of several critical cancer attributes. Furthermore, this 3D reporting methodology can be applied to other organ systems (such as liver) and used to validate radiology imaging modalities.

1353 Improved Interpretation of Immunohistochemistry Stained Pharmocodynamic Biomarkers by Histogram Data Display

JD Deeds, Y Gao, D He, RM Mosher. Novartis Institutes for Biomedical Research, Cambridge, MA.
Background: Immunohistochemistry (IHC) analysis of pharmacodynamic (PD) markers provides valuable morphologic information but is limited by a lack of standardized methods for quantification. Typically, histopathologists set subjective thresholds for identifying cells that are positive for the presence or absence of a biomarker. Generating continuous data for expression levels across the entire range of expression may assist with interpretation by revealing additional features, improving statistical power, and reducing observer subjectivity.
Design: We examined expression of two biomarkers (pRB and ppRB) using chromagenic IHC stained xenograft tumor samples from compound treated animals. Samples were collected at various time points following compound administration. Staining intensity of nuclei was determined using ImageScope and IHC-Nuclear software (Aperio Technologies). Counts of number of nuclei staining for each of 256 intensity levels was computed for each sample.
Results: Examination of the full spectrum of intensity values revealed many aspects not observed via single threshold cutoffs. In the pRB stained samples, we were able to select any of a wide range of threshold values and observe all treatment-related changes. In addition, at one time point the histogram revealed that there are likely two populations of cells responding differently to treatment. ppRB staining on the other-hand revealed significant overlap between treated and vehicle samples, making intra-group comparisons difficult. Small changes in selected threshold values resulted in large changes in treated versus vehicle ratios.
Conclusions: Manual selection of thresholds is subjective and prone to bias. Varying a single threshold can result in different fold changes in experimental samples relative to control samples. Visualizing the continuous range of expression data has numerous advantages: 1) Histograms can indicate when values are well distributed over the measurable dynamic range. 2) Histogram analysis can reveal multiple subpopulations of cells within a sample which may be behaving differently. 3) Better measures of statistical significance may be obtained by analyzing histograms. Selecting optimal thresholds based on histogram analysis may provide better interpretation of changes of PD markers.

1354 Automated Image Analysis of Cytoplasmic Immunohistochemical Stains: A Technique To Overcome Thresholding Challenges

D Gui, G Gerney, N Doan, G Cortina, S Ohsie, J Said, S Dry. UCLA, Los Angeles.
Background: Quantitative immunohistochemical analysis may be more efficient and reproducible than manual interpretation. Unfortunately, image segmentation/thresholding does not work as well for cytoplasmic staining. The brown diaminobenzidene (DAB) chromogen contains red, blue and yellow hues; hematoxylin, the usual counterstain, is blue. When hematoxylin-counterstained images are thresholded for DAB, resulting masks include nonspecific areas, due to the blue component that is part of the DAB brown. No-counterstained images may improve accuracy of quantitative IHC for DAB labeled cytoplasmic antigens.
Design: Three small bowel samples (one section per sample) were analyzed. Initially, the slides were stained for serotonin (DAB) with no-counterstain (NC) and scanned; then they were counterstained with hematoxylin (HC) and scanned again. Scanning was performed at 20x using an Aperio XT wholeslide scanner. The area of cytoplasmic stain and total tissue stained was analyzed using Metamorph software (v 7.0.r4). Five 20X fields per case (15 areas total) were analyzed. The identical areas were analyzed with DAB-NC and DAB-HC.
Results: The automated total measured area was about twice the size using HC compared to NC (17833.14 mm^2 for HC vs. 9425.99 mm^2 for NC). The number of positive cells was identical by manual counts in both groups (n=205). The difference in area counted by the computerized analysis was statistically significant (t-test, p value = 0.002). Since the exact same areas were analyzed with and without HC, the difference in automated measured area can be attributed to thresholding error.
Conclusions: Use of no-counterstained (NC) images improves accuracy of image analysis for cytoplasmic immunostains that use the DAB chromogen. These findings are important for researchers performing quantitative immunohistochemistry.

1355 User Experience with the Online Virtual Rotation in Pathology Informatics: Pretest and Posttest Results

HP Kang, JM Hagenkord, FA Monzon, AV Parwani. Roswell Park Cancer Institute, Buffalo, NY; University of Pittsburgh, Pittsburgh, PA; Creighton University, Omaha, NE; The Methodist Hospital, Houston, TX.
Background: Pathology informatics is increasingly recognized as an important component of pathology training, and efforts are being made to provide informatics training in residency programs and also standardize the scope and objectives of this training. Some of the factors limiting this process are: 1) many programs have limited access to pathology informatics expertise and resources, 2) it is difficult to fit an informatics rotation into an already crowded schedule, and 3) existing informatics training at one institution cannot be easily emulated by other programs due to incompatible rotation structures. We previously presented the 'Virtual Rotation in Pathology Informatics', which was designed with the goal of overcoming these limitations. As an update, we will present our experience with this resource and the usage statistics.
Design: The course includes didactic lectures (captured as audio PowerPoints) given by experts in the field and video-recorded hands-on laboratories. It is supplemented by readings from the textbook 'Practical Pathology Informatics: Demystifying Informatics for the Practicing Anatomic Pathologist' by John Sinard (Springer, 2005). Because it is self-paced, it can accommodate various rotation structures. Module topics and depth of coverage are directed at the level of general practicing pathologist, with quizzes provided for each module. Pre-test and post-test are based on the quizzes. Course progress, as well as completion of the pre-test, post-test, and course survey, can be tracked on the website by an administrator for each institution.
Results: The course is web-based and is hosted and maintained at our institution. There are currently 31 users from 5 institutions, including administrators. The current statistics for trainees are 57.4% correct answers on the pre-test and 81.7 on the post-test for an average increase after the course of 24.3%.
Conclusions: The experience so far with this resource has been positive and it seems to be effective in improving resident competency in pathology informatics and basic computer skills. This free, web-based, self-paced, auto-graded virtual rotation overcomes many of the major limitations pathology residency programs encounter when trying to implement informatics training. It also streamlines much of the record keeping in evaluating the progress and performance of trainees.

1356 Digital Imaging and Its Applications for Cytopathology at a Large Academic Multi-Institutional Center

WE Khalbuss, AV Parwani. UPMC, Pittsburgh, PA.
Background: Digital pathology is increasingly being used in cytopathology practices. We provide our experience in the various practical uses as it relates to digital images such as whole slide imaging for cytopathology practice. We also discuss the logistical and technical concerns for implementing such technologies.
Design: Static "snapshot" images are captured at microscopes workstations. SPOT Insight digital cameras capture both microscopic images at more than thirty locations at six different locations. These static images can be integrated into our APLIS (CoPath Plus).The Zeiss and Aperio Scanscope scanners are used to scan entire whole slides.

With capture, image file sizes are approximately 2.7 GB. Conferences use telepathology through webcast or transmission with the Tandberg video system. On site evaluation in fine needle aspiration can be made remotely through robotic means via robotic microscopy.
Results: Thousands of static images have been captured, using 70 GB of server storage space. Static images are used for teaching, CPC conferences, publications, image-enhanced reporting, and consultation. We have a repository of hundreds of whole slide images; categorized and available through a centralized web-based portal. Selected whole slide images can be accessed remotely by residents and fellow for weekly unknown conferences. Pap smears with potential cervical cytology risk management and false negative and false positive non-gynecological cytology cases can now made available for educational reviews as virtual microscopic slides. Telepathology has been integral to our educational conferences given our institutional geography. Conferences are video recorded with live broadcasts which permit remote attendance via the internet. More than 1000 conferences have been archived since 2002. Robotic telepathology is being used by cytopathologists for on site evaluation of fine needle aspirates.
Conclusions: Digital pathology has been successfully used in cytopathology for teaching, CPC conferences, QA/QC, publications, image-enhanced reporting, consultation, retrospective case review, and remote FNA evaluations. Future goals and development in digital pathology include image capture and image analysis especially with immunohistochemistry and FISH.

1357 @-Pathology and Prostate Cancer: The Experience of the French Uropathology Club

V Moline, H Baumert, W Majoub, A Balaton, E Brunet. Hopital Saint Joseph, Paris, France; CCITI, Dijon, France.
Background: Use of virtual slides system and web based technologies in pathology is promising, but many pathologists remain sceptical about the feasibility or reproducibility of diagnosis based on analysis of digitally scanned slides. Sending slides from difficult cases to a panel of expert is time-consuming with a risk of loss, damage or breakage of the slides. We conducted an evaluation on digitally scanned slides of prostate biopsies to assess reproducibility of the diagnosis of prostate cancer and different histological predictive features such as Gleason's score, length of tumor, nervous invasion.
Design: 650 slides from 50 prostate biopsies were prospectively retrieved from the files of 10 French pathology databases. Each pathologist retrieved the 5 first cases of June 2008, and sent all the slides to the centralization laboratory. All the slides were scanned on Zeiss scan system and digital images were retrieved on a server based in Dijon France. Each pathologist received an electronic copy of the program file, with a prostate biopsy user manual to download the CCITI system. The experts had access to clinical information before they blindy reviewed the virtual slides. For each case they had to fill out a score sheet and select a list of Gleason's score on which the diagnosis was based. Each expert had to justify the Gleason's score on which he or she make the diagnosis by selecting region of interest (ROI) using a drawing tool. Interobserver agreement on the diagnosis was calculated according to the Kappa test.
Results: 90% of the analyses were performed at time. There was a general good agreement on the diagnosis of prostate cancer. The exact agreement of Gleason's score was observed in 78% of the cases. Problems encountered with the software and the slides review system was evaluated. The ROI was extremely useful to understand discrepancy between the experts.
Conclusions: Our results showed that @-web based pathology is extremely useful tool and promising for the interpretation of prostate cancer on biopsies and in case of difficulty the CCITI system is a useful start for the creation of virtual slide library for a group of expert in uropathology.

1358 Development and Use of Laboratory Information System (LIS) Driven Tool for Pre-Signout Quality Assurance of Random Surgical Pathology Reports

AV Parwani, R Dhir, S Yousem, S Kelly, A Piccoli, L Wiehagen, K Lassige. UPMC - Shadyside Hospital, Pittsburgh, PA.
Background: In many institutes, all or a subset of cases are reviewed routinely by a second pathologist as a method of quality assurance (QA). Studies have shown that error rates range from 0.26% to 1.2% for global in-house prospective review and 4.0% for retrospective review. The aim of the current study was to develop a Pre-Signout Quality Assurance Tool (PQAT) which allows the LIS to randomly select 5% of cases for QA and send that case to the QA pathologist for review.
Design: Several vendor-assisted software modifications were done to our existing LIS application, CopathPlus. These modifications and the design of the new PQAT takes into account our existing workflows. The "blinded" signout pathologist will have a case randomly selected 5% of the time prior to signout. As soon as the case is selected and with the knowledge of the primary pathologist, the case is sent to a QA work list where an assigned QA pathologist reviews the case and either agrees or disagrees with the original diagnosis and enters their comments into the LIS. At this point the case is returned to the original pathologist and it is signed out.
Results: The first version of PQAT has been built and tested for review of GenitoUrinary Pathology cases. When the pathologist presses the Signout button, surgical pathology cases are considered for QA selection. Cases selected for QA are routed to the QA Work list. The QA pathologist reviews all cases on this work list and enters a new QA review. The case is then sent to the original pathologist's signout work list. Agreement level is displayed on the work list so that the original pathologist must review the QA findings and resolve discrepancies with his/her diagnosis. The QA comments and review is strored in the LIS and is not displayed on the surgical pathology report. The tool and existing workflow has been tested on multiple cases in our test LIS system. The percentage of cases for QA can be modified according to requirements and this tool can be expanded to all surgical pathology benches.
Conclusions: Since we are a subspecialty-based sign out practice, we routinely do not have a second prospective review of cases. The PQAT and the designed workflow allows for corrective action and re-review of randomly selected cases, prior to signout. This tool will also result in real time QA rather than a retrospective QA process. The PQAT will also allow for focused QA based on the difficult or controversial areas of the subspecialty.

1359 Validation of an Inexpensive Telepathology System for Frozen Section Diagnosis

SJ Sirintrapun, MJ Schniederjan, S Logani, AB Carter. Emory University, Atlanta, GA.
Background: Emory Neuropathology is housed within Emory University Hospital (EUH). In June 2007, a neurosurgical practice began at Emory Johns Creek Hospital (EJCH) with about 5 frozen sections (FS) per month. The distance between EJCH and EUH (21.9 mi) prompted development of a telepathology consultation service. CapSure (GlobalMedia) was selected for its low cost ($16,500) and good image quality.
Design: The system has a microscope-mounted digital camera and networked computer which project live images to the EUH viewing station using web conferencing software (GoToMeeting). A pathologist is present at EJCH to drive the slide under the microscope. Patient identifiers are related via telephone only. The system was validated using 17 previous neuropathology FS cases. Each NP was provided with only the patient's age, gender, specimen and clinical history. Concordance between the CapSure FS diagnosis to the rendered final diagnosis was determined according to Horbinski et al (*J Neuropathol Exp Neurol* 2007;66:750-9). Costs of the system were also evaluated.
Results: The validation results are listed in Table 1.

Table 1. Concordance of CapSure FS Diagnosis to Final Diagnosis.

Diagnosis	# Cases	E	EC	D	Comments
Reactive Gliosis	1		3/3		
Meningioma	4	11/11			1 evaluated by 2 NPs
Ependymoma	1	2/3		1/3	D: meningioma
Schwannoma	1	3/3			
Anaplastic Astrocytoma (WHO Grade III)	1		3/3		
Glioblastoma Multiforme (WHO Grade IV)	4	5/12	6/12	1/12	D: radiation necrosis
Pituitary adenoma	1	3/3			
Metastatic Carcinoma	2	6/6			
Metastatic Sarcoma	1	2/2			Evaluated by only 2 NPs
High Grade Lymphoma	1		2/3	1/3	D: multiple myeloma
VALIDATION TOTAL	**17**	**32/49 (65.3%)**	**14/49 (28.6%)**	**3/49 (6.1%)**	**E + EC = 93.9%**

Category assignment / total number of examinations. None were deferred. E: Exact; EC: Essentially Concordant; D: Discrepant (Horbinski et al).

The cost of a NP commuting to EJCH for on-site FS diagnosis is estimated to range between $800-1400 per month and $9600-16,800 per year.
Conclusions: CapSure provides an inexpensive mechanism for telepathology as compared to other telepathology systems and is estimated to pay for itself in 1-2 years. Disadvantages are the required participation of an EJCH pathologist and the NP's lack of direct slide control. Of the 3 discrepant diagnoses, the most concerning is the false negative. The remaining misclassifications were unlikely to be clinically significant. Concordance rates are similar to those reported with other systems. *Note: No financial or other support was received from any vendor for this project.

1360 3D Microscopic Anatomy Using Whole Slide Imaging (WSI)

Y Yagi, AR Sohani, M Mino-Kenudson, JR Gilbertson. Harvard Medical School, Boston, MA.
Background: In the past, most 3D imaging in Pathology was done from a single slide using multiple focal planes (confocal microscopy or cytology) or through volume rendering of large, macro structures on multiple physical sections. However, WSI technologies and rendering software have now improved to the point that 3D reconstruction of large structure at microscopic scale from hundreds of serial sections is possible. The challenges in this approach include section registration, quality of tissue, effects of tissue processing and sectioning, and the huge amount of data that can be generated.
Design: Specimens included lymph node, pancreas and mouse embryo. 66-100 serial sections were cut manually or by an automated sectioning machine (AS-200, KURABO INDUSTRIES LTD. Japan) from formalin-fixed paraffin-embedded blocks and stained with H&E. Serial sections were scanned at 0.33/pixel using a Mirax Scan device (3DHISTECH Ltd, Carl Zeiss Microimaging GmbH). 3D reconstruction was done using Mirax software. WSI were aligned to produce a 66-100 section 3D stack that could be subsampled, sectioned in various planes, freely rotated to expose 3D relationships in tissue. Spacing between scanned sections was varied dynamically during the analysis to explore specific features.
Results: Morphologic features were often enhanced upon 3D reconstruction, although the relatively low resolution of the 3D model precluded extensive analysis of cellular interactions. The reconstruction process was made more difficult by tissue processing effects such as wrinkle, stretch, bubble, variable thickness across the tissue section. Figure 1 and 2 show full and cut models of mouse embryo and pancreas

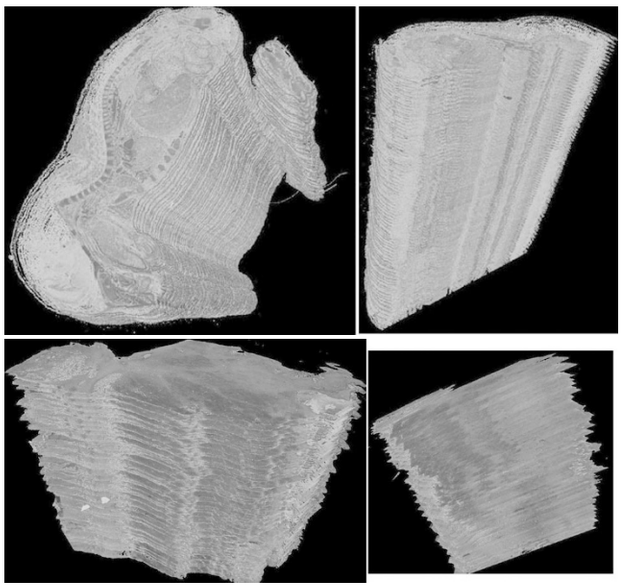

Conclusions: 3D reconstruction from multiple serial WSI sections can be used to generate impressive views of tissue. In the future this technique could be an important aspect of pathology analysis. However, we need to overcome many challenges to make this are routine process.

Kidney

1361 Segmental Sclerotic Lesions in Transplant Kidney: Insights in the Diagnostic Dilemma

M Asgari, AM Gomes, AB Fogo. Iran University of Medical Sciences, Tehran, Islamic Republic of Iran; Centro Hospitalar de Vila Nova de Gaia, Oporto, Portugal; Vanderbilt University Medical Center, Nashville, TN.

Background: Segmentally sclerotic glomeruli in the transplant (Tx) kidney may be due to recurrence of FSGS (Rec FSGS), or occur secondarily (Sec FSGS), e.g. related to hypertension, chronic allograft nephropathy, chronic Tx glomerulopathy or calcineurin inhibitor (CNI) toxicity. We examined nonimmune complex segmental sclerosing lesions in Tx, and classified based on clinical findings, time of diagnosis after Tx, light microscopic and EM findings.

Design: All Tx biopsies with segmental sclerosis and/or extensive foot process effacement (FPE) and negative IF from 1995 till 2006 were reviewed, excluding Tx glomerulopathy. All slides, reports, EM photomirographs, clinical history and follow-up were reviewed. Light microscopic (LM) findings were classified by the Colombia schema. Findings of Sec FSGS such as CNI toxicity, expanded lamina rara interna and limited FPE were assessed, and cases classified as Rec vs Sec FSGS.

Results: Fortytwo patients (29 male, 13 female) met entry criteria. Average age was 37±14 years (range 11 to 56). Twenty patients (48%) were African American and 13 (31%) were Caucasian. Twentythree (55%) had nephrotic proteinuria at the time of biopsy. Biopsy interval ranged from 4 days to 8 years after Tx. Twentythree (54%) case were classified as Rec FSGS, 15 (35%) as Sec FSGS and 4 (10%) as likely de novo FSGS. Ten (54%) Rec FSGS cases showed only extensive FPE, four (17%) cellular (CELL), four (17%) collapsing (COLL), and four (17%) not otherwise specified (NOS) lesions. In cases classified as likely Sec FSGS, NOS lesion was the most common morphologic variant, in 6 (40%), followed by 3 (20%) COLL, 2 (13%) CELL and 3 (20%) with FPE and other features of Sec FSGS. Rec FSGS was most common in early biopsies (85% of all FSGS cases in first 6 months). In contrast, 13 (65%) biopsies at > 2 years showed Sec FSGS. Nearly all patients, whether Rec or Sec FSGS, lost their kidney during the following months to years.

Conclusions: Early time of recurrence and extensive FPE were characteristic of Rec FSGS. NOS variant is more common in Sec FSGS, whereas extensive FPE alone is the most common finding in Rec FSGS. COLL, related to CNI toxicity, and CELL lesion can be seen in both Rec and Sec FSGS. We conclude that integrated analysis of LM, EM and clinical data help to differentiate varying etiologies of sclerotic lesions in the Tx.

1362 Coumadin Overdose Accompanied by Acute Tubular Injury: Pathological Findings in Renal Biopsies

SV Brodsky, A Satoskar, J Chen, G Nadasdy, L Hebert, T Nadasdy. Ohio State University, Columbus, OH; New York Medical College, Valhalla, NY.

Background: Warfarin therapy has been associated with microscopic and gross hematuria. However, acute renal injury in these patients has been rarely described.

Design: Herein we report pathological findings in renal biopsies in patients with coumadin overdose and acute renal dysfunction.

Results: Seven renal biopsies from patients on coumadin therapy with gross hematuria were found in our database from 2004 till 2008. Mean age was 65.8±6.2 years. There were four males and three females. All patients had an increased INR (4.5±1.5 IU) and elevated serum creatinine (4.2±0.98 mg/dl)) at the time of biopsy, versus 1.3±0.41 mg/dl baseline levels. Four patients had proteinuria. Morphologically, all renal biopsies revealed red blood cells (RBC) in Bowman's space, RBC casts in tubules and acute tubular injury (ATI). Patients did not have history of extra-renal causes of ATI or underlying renal diseases resulting in gross hematuria. Hematuria was resolved after normalization of INR. Depletion of vitamin K in mice resulted in hematuria, but no tubular RBC casts and ATI, suggesting that an underlying renal condition is necessary for the development of RBC casts.

Conclusions: Occlusive RBC casts with acute tubular injury is a possible serious complication of a warfarin overdose and physicians should be aware of it.

1363 De Novo Membranous Glomerulonephritis Is Associated with C4d Depostion in Peritubular Capillaries and Basement Membrane Multilamination: Putative Variant of Chronic Humoral Rejection

AB Collins, AB Farris, W Wong, S Saidman, N Tolkoff-Rubin, NB Goes, DS Ko, AB Cosimi, RB Colvin. Massachusetts General Hospital, Boston, MA.

Background: The pathogenesis of de novo MGN in renal allografts is unknown. Animal studies support a role for non-MHC glomerular alloantigens. In a recent case report, the onset of de novo MGN correlated with development of anti-donor specific antibodies (DSA). Here we test the hypothesis that de novo MGN is a variant of chronic humoral rejection.

Design: All cases of de novo MGN and other forms of glomerular disease with available tissue were studied from transplant biopsies (1997-2008), C4d deposition (immunofluorescence) and electron microscopy. During this time C4d+ CHR was diagnosed on 8.4% of 738 transplant biopsies.

Results: De novo MGN had a higher frequency of C4d+ than the other de novo GN combined (p=0.017). Only de novo hepatitis C virus (HCV) GN was associated with C4d. Recurrent MGN and HCV were not statistically different from de novo. C4d+ de novo MGN commonly had mulitlamination of the GBM (4/4) and PTC BM (3/4), but this was not statistically greater than in C4d- de novo MGN (1/6 and 1/5 respectively; p>0.05). All de novo MGN patients tested for HLA-DSA were positive (3 class I, 1 also class II). One patient had three biopsies over 4 years all with de novo MGN, but C4d was present only in the last biopsy. One C4d- case had an earlier biopsy with focal C4d (10%).

Diagnosis	N Pts	C4d+ PTC	%C4d+
De novo MGN	16	6	38%
De novo FSGS	15	0	0%
De novo IgA	4	0	0%
De novo HCV	5	2	40%
De novo Misc GN	5	0	0%
Recurrent MGN	6	1	17%

Conclusions: C4d+ in PTC, the hallmark of CHR, is strongly associated with de novo MGN, but not other de novo GN except for that of HCV. The lack of a tight association argues that different antigens are the target of de novo MGN and CHR and fits with experimental data suggesting that non-MHC alloantigens may be the target. The association may be due to a propensity to form alloantibodies of any type or promotion of an immune response to glomerular antigens secondary to injury mediated by HLA antibodies. In any case, this study supports the concept that de novo MGN may be a variant of CHR.

1364 Challenges in the Diagnosis of Chronic Antibody Mediated Rejection Due to Loss of Peritubular Capillaries and Low Extent and Transient Nature of C4d Deposition

AB Collins, AB Farris, RN Smith, CD Adams, PA Della Pelle, S Saidman, W Wong, RB Colvin. Massachusetts General Hospital, Boston, MA.

Background: The diagnosis of acute antibody mediated rejection (AMR) is based on C4d deposition in >50% of peritubular capillaries (PTC). However, a loss of peritubular capillaries has been reported in late graft biopsies. Here we test whether the same criteria of C4d extent are appropriate for chronic AMR.

Design: All available cases of chronic humoral rejection (CHR) (1997-2008) were stained with two color immunohistochemistry for CD34 and C4d and compared with transplant glomerulopathy and no C4d (TG C4d-), chronic calcineurin inhibitor toxicity (CNIT), and normal transplant biopsies (NT). PTC density was quantitated visually and by morphometry (Aperio) and correlated with graft function and fibrosis (morphometry).

Results: Biopsies with CHR or TG C4d- had significantly reduced PTC density compared with NT (Table). Within the CHR group, the density of C4d+ PTC correlated with the overall capillary density (p=0.001). There was a wide spectrum of the % of PTC with (1-90%). Most cases (9) were Banff C4d2 (10-50%); a minority (7) were C4d3 (>50%). Most CHR cases had glomerular capillary wall C4d deposition (83%). The % fibrosis correlated with the Cr at the time of biopsy (p=0.04). C4d%+ and PTC density showed no statistically significant correlation with Cr at the time of the biopsy. PTC density was decreased with time post-transplant. Our data suggest that some TG C4d- cases are the sequelae C4d+ lesions, since 2/7 had had prior acute AMR. Furthermore one of the C4d+ CHR cases had a later biopsy that was TG C4d-. All of the CHR recipients tested had donor specific antibody (5 class I only, 6 class II only and 2 both), including the one with 1% C4d+ PTC and C4d+ glomeruli. Aperio microvascular counts were highly correlated with visual counts (r=0.928), although they were consistently higher.

			Capillary Density/mm2			CD34/mm2
Diagnosis	N	yrs post tx	CD34	C4d	%C4d+	p vs NT
CHR	17	9.2±6.1	228±108	109±113	44±33%	<0.03
TG C4d-	7	13.9±12.6	165±138			0.006
CNIT	6	5.2±3.2	243±185			n.s.
NT	7	0.4±0.7	319±188			